

A Microwave Study of the Ammonia–Nitric Acid Complex

M. E. Ott[†] and K. R. Leopold*

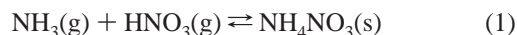
Department of Chemistry, University of Minnesota, Minneapolis, Minnesota 55455

Received: October 26, 1998; In Final Form: January 6, 1999

Microwave spectra of $\text{H}_3^{14}\text{N}-\text{H}^{14}\text{NO}_3$, $\text{H}_3^{15}\text{N}-\text{H}^{14}\text{NO}_3$, $\text{H}_3^{14}\text{N}-\text{H}^{15}\text{NO}_3$, and $\text{H}_3^{14}\text{N}-\text{D}^{14}\text{NO}_3$ have been obtained by Fourier transform spectroscopy in a supersonic jet. The spectra are consistent with a hydrogen-bonded structure having a planar arrangement of the heavy atom frame and a linear or near-linear hydrogen bond involving the HNO_3 proton and the lone pair on the ammonia. The hydrogen bond length obtained from the rotational constants is 1.736(63) Å and the nitrogen–nitrogen separation is 3.344(12) Å. The NO single bond of the nitric acid and the C_3 axis of the NH_3 form angles of 54(4)° and 21(3)°, respectively, with the line joining the centers of mass of the monomers. The hydrogen bond length is significantly shorter than that observed in related complexes such as $\text{H}_3\text{N}-\text{HCl}$ and $\text{H}_3\text{N}-\text{HBr}$, indicating a particularly strong interaction between ammonia and nitric acid.

Introduction

For many years, the reaction



has been a subject of considerable interest in atmospheric modeling.^{1–5} Ammonium nitrate can be a significant component of continental aerosol, and as such, its formation in the troposphere has a broad impact on both climate and the heterogeneous chemistry of atmospheric trace gases. Moreover, its deposition provides a significant means of transferring nitrogen out of the atmospheric nitrogen cycle and back into the biosphere. Thus, it is not surprising that the formation and thermodynamics of ammonium nitrate continues to be the subject of both field and laboratory investigations.^{6–10}

From the standpoint of fundamental chemistry, reaction 1 is also important as a prototypical example of a Brønsted acid–base reaction. An interesting question about this system concerns the extent to which the presence of solvent is necessary to foster the formation of the ion pair, $\text{NH}_4^+\text{NO}_3^-$. This issue has a long history of investigation,^{11,12} dating back to early matrix isolation work by Ritzhaupt and Devlin.¹¹ The general problem of the stabilities of ion pairs vs hydrogen-bonded complexes, particularly with regard to the influence of a crystalline or matrix environment, goes back even further.¹³ In the case of $\text{H}_3\text{N}-\text{HNO}_3$, experimental studies¹¹ indicate that in an argon matrix at ~10 K, the ion pair ($\text{NH}_4^+\text{NO}_3^-$) forms in the absence of any aqueous solvation. This observation forms an interesting contrast with that for the nitric acid–water system, in which $\text{H}_3\text{O}^+-\text{NO}_3^-$ is stabilized only with greatly increased concentrations of water in the matrix. The question of what *chemical constituency* is required to give rise to ion pair formation in the *gas phase* has been thoroughly investigated by Legon and co-workers in the complexes $\text{R}_3\text{N}-\text{HX}$.¹⁴

Recent theoretical work by Tao et al.^{15–17} has provided a particularly detailed view of the effect of solvation on proton transfer. For $\text{H}_3\text{N}-\text{HNO}_3$, for example, structures and binding

energies have been computed for the complexes $\text{H}_3\text{N}-\text{HNO}_3-(\text{H}_2\text{O})_n$ for values of $n = 0, 1, 2$, and 3.¹⁶ The results indicate that with $n = 0$ or 1, $\text{H}_3\text{N}-\text{HNO}_3$ is a hydrogen-bonded species but with $n \geq 2$ the system becomes a solvated ammonium nitrate ion pair.

Despite the significant interest in the nitric acid–ammonia system, it appears that there has been no gas-phase spectroscopy of the NH_3-HNO_3 complex. Thus, in this paper, we present a microwave study of this species. Our results support the hydrogen-bonded structure predicted theoretically^{15,16,18} and, moreover, should establish a useful benchmark for possible future spectroscopic investigations.

Experimental Section

Rotational spectra of $\text{H}_3\text{N}-\text{HNO}_3$ were obtained using a pulsed nozzle Fourier transform microwave spectrometer,¹⁹ which has been described previously.²⁰ Since nitric acid and ammonia react rapidly in bulk, a “co-injection” source²¹ was used to generate the complex transiently during the expansion. Argon at a pressure of 1.7 atm was passed over 90% HNO_3 and introduced into the vacuum chamber via a pulsed solenoid valve directed along a line perpendicular to the axis of the microwave cavity. Pure ammonia at a backing pressure of 0.33 atm was continuously introduced through a 0.007 in. i.d. stainless steel needle situated several millimeters downstream of the nozzle orifice. In this way, the complex was produced without appreciable deposits of solid ammonium nitrate, and in sufficient quantity to yield excellent signal-to-noise ratios on most transitions observed.

Spectra of $\text{H}_3^{14}\text{N}-\text{H}^{15}\text{NO}_3$, $\text{H}_3^{15}\text{N}-\text{H}^{14}\text{NO}_3$, and $\text{H}_3^{14}\text{N}-\text{D}^{14}\text{NO}_3$ were observed using isotopically enriched samples. $^{15}\text{NH}_3$ was obtained commercially, but the H^{15}NO_3 was synthesized “in house” by reacting approximately 2.0 g of $\text{Na}^{15}\text{NO}_3$ with 3.5 mL of H_2SO_4 .²² The latter was used in excess in order to keep the final product dry. The resulting H^{15}NO_3 was distilled at approximately 75 °C, and a yield of approximately 1 mL was obtained. For experiments involving DNO_3 , a similar procedure was followed, with dry D_2SO_4 (>98%) used in place of H_2SO_4 .

* To whom correspondence should be addressed.

[†] Present address: Western Wyoming Community College, P.O. Box 428, Rock Springs, WY 82902-0428.

TABLE 1: Assigned Transitions of H₃N–HNO₃ and H₃N–DNO₃^{a,b}

transition	I''	F''	I'	F'	H ₃ N–HNO ₃	H ₃ N–DNO ₃	transition	I''	F''	I'	F'	H ₃ N–HNO ₃	H ₃ N–DNO ₃
0 ₀₀ –1 ₀₁	1	1	1	0	4851.431(+0.002)		1 ₁₀ –2 ₁₁	2	2	2	2	10163.421(–0.006)	10073.041(–0.004)
	2	2	2	2	4851.506(–0.003)			1	0	1	1		10073.055(+0.004)
	0	0	0	1	4851.552(+0.002)			2	2	2	3	10163.460(–0.001)	10073.077(–0.001)
	1	1	1	2	4852.057(–0.001)			2	2	2	1		10073.238(+0.010)
	2	2	2	3	4852.138(+0.001)			0	1	0	2		10073.265(–0.005)
	1	1	1	1	4852.195(+0.001)			2	3	2	3		10073.593(+0.000)
1 ₁₁ –2 ₁₂	2	2	2	1	4853.020(–0.001)			1	1	1	1	10164.007(–0.001)	
	1	0	1	1	9243.361(–0.008)	9160.066(+0.008)		1	2	1	3	10164.007(+0.003)	10073.621(–0.004)
	2	2	2	2	9243.361(+0.000)	9160.052(+0.000)		1	2	1	2		10073.687(–0.010)
	2	2	2	3	9243.392(+0.002)	9160.085(+0.006)		2	3	2	4	10164.094(+0.002)	10073.719(+0.009)
	2	3	2	2	9243.479(–0.004)			1	1	1	2	10164.140(+0.000)	10073.751(–0.005)
	1	2	1	1		9160.182(+0.004)		2	1	2	1	10164.871(+0.005)	10074.499(+0.009)
	2	3	2	3	9243.512(+0.000)	9160.202(+0.003)		2	1	2	0	10164.924(–0.002)	10074.557(+0.009)
	1	1	1	1	9243.563(+0.003)	9160.248(+0.003)	2 ₁₂ –3 ₁₃	2	4	2	4	13855.327(+0.000)	13730.429(+0.008)
	1	2	1	3	9243.975(+0.008)	9160.650(–0.011)		1	2	1	2	13855.327(–0.004)	
	2	3	2	4	9244.058(+0.006)	9160.746(+0.003)		2	2	2	3	13855.834(+0.005)	13730.926(–0.002)
	1	2	1	2		9160.721(–0.005)		2	3	2	4	13855.866(–0.002)	13730.962(–0.003)
	1	1	1	2	9244.107(+0.002)	9160.798(+0.005)		1	1	1	2		13730.982(+0.009)
	2	2	2	1	9244.195(+0.000)			2	1	2	2	13855.974(+0.004)	13731.074(+0.004)
1 ₀₁ –2 ₀₂	0	1	0	2	9244.222(–0.010)	9160.926(–0.001)		1	3	1	4	13856.026(+0.004)	13731.122(+0.000)
	2	1	2	1	9244.474(+0.003)	9161.160(–0.003)		2	4	2	5	13856.054(–0.001)	
	2	1	2	0	9244.534(+0.000)	9161.211(–0.012)		1	2	1	3	13856.054(–0.005)	13731.152(–0.006)
	1	1	2	2	9687.368(+0.006)			2	1	2	1		13731.171(+0.001)
	2	3	2	2		9600.618(–0.015)	2 ₀₂ –3 ₀₃	1	3	1	3		13731.213(–0.009)
	1	1	1	1	9687.459(+0.005)	9600.668(+0.001)		1	2	1	2		14361.858(+0.003)
	2	3	2	3	9687.480(–0.002)	9600.699(+0.005)		2	4	2	4	14491.745(–0.001)	14361.873(+0.008)
	2	1	2	1	9687.552(–0.003)	9600.752(–0.018)		2	1	2	2	14492.287(+0.002)	
	1	2	2	3	9687.568(+0.006)			2	0	2	1		14362.431(+0.010)
	2	1	2	0	9687.686(–0.002)			0	2	0	3	14492.331(+0.004)	14362.448(–0.002)
	1	2	1	1		9600.785(–0.013)		2	2	2	3	14492.379(+0.000)	14362.504(+0.002)
	2	2	2	2	9688.042(–0.005)	9601.257(–0.005)		2	3	2	4	14492.401(–0.009)	14362.522(–0.009)
	1	2	1	3		9601.342(+0.005)		1	3	1	4	14492.427(–0.003)	14362.554(+0.000)
	1	1	1	2	9688.128(–0.002)	9601.342(–0.003)		2	4	2	5	14492.444(+0.004)	14362.568(+0.004)
	2	3	2	4	9688.144(–0.001)	9601.373(+0.013)		1	3	1	3	14492.578(+0.002)	14362.684(–0.010)
	1	0	1	1	9688.217(–0.002)		2 ₁₁ –3 ₁₂	1	3	1	4	15235.558(+0.000)	
	1	2	1	2	9688.268(+0.002)	9601.475(+0.000)		0	2	0	3	15235.569(+0.001)	
	2	2	2	1	9689.060(–0.008)			2	4	2	5	15235.593(–0.003)	
	0	1	0	2	9689.082(+0.005)	9602.308(+0.011)		2	1	2	1	15235.701(+0.007)	
								1	3	1	3	15235.739(+0.001)	
								2	2	2	2	15235.765(–0.005)	

^a All frequencies are in MHz. Measurement uncertainties are estimated to be 5 kHz for the HNO₃ complex and 10 kHz for the DNO₃ complex. Numbers in parentheses are the residuals from the least squares fits. ^b **I**₁ + **I**₂ = **I**; **I** + **J** = **F**.

Results

a-type rotational transitions were observed for H₃¹⁴N–H¹⁴NO₃, H₃¹⁴N–H¹⁵NO₃, H₃¹⁵N–H¹⁴NO₃, and H₃¹⁴N–D¹⁴NO₃ (Tables 1 and 2). ¹⁴N hyperfine structure was observed and analyzed using standard methods for one or two nuclei, as appropriate.²³ In the DNO₃ complex, the deuterium hyperfine splittings were poorly resolved and were not analyzed. Spectra of H₃¹⁵N–H¹⁴NO₃ were first fitted to eQq_{aa}, (eQq_{bb} – eQq_{cc}), and a series of hyperfine-free line centers, and the resulting quadrupole coupling parameters were used as a guide to assigning the more complex spectrum of the H₃¹⁴N–H¹⁴NO₃ species. Over 60 hyperfine frequencies in the parent derivative were readily assigned, though for many states, the particular quantum number assignments were found to be sensitive to the value of (eQq_{bb} – eQq_{cc}). This occurs when the |J, I₁, I₂, I, F⟩ eigenfunctions are strongly mixed and the dominant contribution (from which the state label is derived) changes as (eQq_{bb} – eQq_{cc}) is varied. The resulting “quantum number flipping” turned out to be problematic during the search for the least squares minimum, and thus, in the final fit of the H₃¹⁴N–H¹⁴NO₃ data, the value of (eQq_{bb} – eQq_{cc}) for the HNO₃ nitrogen was constrained to the 0.025 MHz value determined for H₃¹⁵N–H¹⁴NO₃. Such a constraint is reasonable since the ¹⁴N/¹⁵N isotopic substitution produces only a small rotation of the inertial axes. The same constraint was applied in treating

the H₃N–DNO₃ data. Line centers are listed in Table 3, and the quadrupole coupling parameters are given in Table 4. A sample spectrum is shown in Figure 1.

The hyperfine-free line centers for each isotopomer were next fitted to Watson’s Hamiltonian for a distortable asymmetric rotor,^{23b} viz.,

$$H = [(B + C)/2 - \Delta_J \mathbf{J}^2] \mathbf{J}^2 + [A - (B + C)/2 - \Delta_{JK} \mathbf{J}^2 - \Delta_K \mathbf{J}_z^2] \mathbf{J}_z^2 + [(B - C)/2 - 2\delta_J \mathbf{J}^2] (\mathbf{J}_x^2 - \mathbf{J}_y^2) - \delta_K [\mathbf{J}_z^2 (\mathbf{J}_x^2 - \mathbf{J}_y^2) + (\mathbf{J}_x^2 - \mathbf{J}_y^2) \mathbf{J}_z^2] \quad (2)$$

Here, A, B, and C are the effective rotational constants and Δ_J, Δ_{JK}, Δ_K, δ_J, and δ_K are centrifugal distortion constants. Given the scope of the data, only a subset of the distortion constants was needed to fit the observed rotational transitions. Since only values of K_p = 0 and 1 were observed, Δ_K and δ_K are not determined and were set to zero. Δ_{JK} and δ_J are, in principle, both determinable from the available data, but their dependences are weak and their values are highly correlated. Moreover, attempts to fit the rotational constants simultaneously with Δ_J, Δ_{JK}, and δ_J resulted in singular matrices that caused our least squares fitting routine to fail. After experimenting with several methods of fitting the data, we eventually chose to constrain Δ_{JK} to zero as well and fix δ_J at several trial values from 0 to

TABLE 2: Assigned Transitions of $\text{H}_3^{15}\text{N}-\text{H}^{14}\text{NO}_3$ and $\text{H}_3^{14}\text{N}-\text{H}^{15}\text{NO}_3$ ^{a,b}

transition	F''	F'	$\text{H}_3^{15}\text{N}-\text{H}^{14}\text{NO}_3$	$\text{H}_3^{14}\text{N}-\text{H}^{15}\text{NO}_3$
$0_{00}-1_{01}$	1	1	4705.469(−0.001)	4837.534(−0.001)
	1	2	4705.582(+0.001)	4838.130(+0.001)
	1	0	4705.749(+0.000)	4839.021(+0.000)
$1_{11}-2_{12}$	1	2	8978.008(−0.001)	9218.051(−0.002)
	2	2	8978.069(+0.001)	9218.149(−0.001)
	2	3	8978.124(+0.000)	9218.685(+0.002)
$1_{01}-2_{02}$	1	1		9218.883(+0.000)
	0	1	8978.244(+0.000)	9219.126(+0.001)
	2	2	9396.989(−0.003)	9659.705(+0.001)
$1_{10}-2_{11}$	0	1		9659.818(+0.001)
	1	2	9397.110(+0.006)	9660.298(+0.000)
	2	3	9397.110(−0.002)	9660.351(+0.001)
$2_{12}-3_{13}$	1	1	9397.288(−0.002)	9661.300(−0.003)
	1	2	9843.846(+0.002)	10132.854(−0.002)
	2	2	9843.891(−0.005)	10133.356(+0.003)
$2_{02}-3_{03}$	1	1	9843.944(+0.001)	10133.019(+0.002)
	2	3	9843.963(+0.003)	10133.454(−0.003)
	0	1	9844.073(−0.001)	10134.262(+0.001)
$2_{11}-3_{12}$	3	3	13458.384(−0.003)	
	2	3	13458.446(+0.004)	13817.951(−0.003)
	1	2	13458.473(−0.002)	13818.106(+0.008)
$2_{11}-3_{12}$	3	4	13458.473(−0.002)	13818.138(−0.004)
	2	2	13458.566(+0.004)	
	3	3	14060.584(+0.004)	14450.547(+0.001)
$2_{11}-3_{12}$	1	2		14451.113(+0.002)
	2	3	14060.699(+0.000)	14451.190(−0.003)
	3	4	14060.699(−0.004)	14451.230(−0.001)
$2_{11}-3_{12}$	2	2	14060.866(+0.000)	14452.118(+0.001)
	2	3		15189.772(+0.000)
	3	4		15189.945(+0.001)
$2_{11}-3_{12}$	1	2		15189.982(−0.001)

^a All frequencies are in MHz. Measurement uncertainties are estimated to be 5 kHz. Numbers in parentheses are the residuals from the least squares fits. ^b $\mathbf{F} = \mathbf{I}^{(14}\text{N}) + \mathbf{J}$.

3 kHz while optimizing the remaining parameters, $(B + C)/2$, $(B - C)/2$, $[A - (B + C)/2]$, and Δ_J , for each choice.²⁴ The spectroscopic constants that resulted from the best of such fits for each isotopomer are also listed in Table 4, where the strong correlation between Δ_J and δ_J is evident. The values of the rotational constants, however, were not significantly effected by the choice of δ_J . The residuals of the rotational line centers appear in Table 3.

Following the successful analyses of the a-type spectra, careful searches were conducted for the b-type transitions of the parent species. The spectroscopic constants in Table 4 predict the $2_{12}-3_{03}$ and $1_{01}-1_{10}$ transitions at 5155 and 10 242 MHz, respectively, and thus the regions from 4300 to 6010 MHz and from 9500 to 10 600 MHz were searched under carefully monitored source conditions and with the use of several power levels of the polarization pulse. Despite our best efforts, however, no transitions attributable to the complex could be found. For the structure deduced below, the sum of the NH_3 and HNO_3 monomer moments projects only 0.005 D onto the b-inertial axis of the complex. We presume, therefore, that the apparent absence of b-type transitions arises from a fortuitously near-vanishing value of μ_b .

Due to the proton nuclear spin statistics, both $K = 0$ and $K = \pm 1$ states of ammonia are expected to be populated in the jet. In the limit of free internal rotation of the ammonia within the complex, these correlate with “ $m = 0$ ” and “ $m = \pm 1$ ” internal rotor states, respectively. Nguyen et al.¹⁵ find no evidence of a secondary hydrogen bond involving the NH_3 hydrogens, and indeed, there is little reason to expect a significant barrier to internal rotation in this system.²⁵ Thus, not surprisingly, no evidence was found for the existence of E-state spectra

TABLE 3: Hyperfine-Free Line Centers for $\text{H}_3\text{N}-\text{HNO}_3$ and its Derivatives^a

J''	K_p''	K_o''	J'	K_p'	K_o'	frequency ^{a,b}	(obs − calc) ^c
$\text{H}_3^{14}\text{N}-\text{H}^{14}\text{NO}_3$							
0	0	0	1	0	1	4852.019(2)	0.003
1	1	1	2	1	2	9243.895(1)	−0.005
1	0	1	2	0	2	9688.093(1)	0.004
1	1	0	2	1	1	10163.963(2)	−0.011
2	1	2	3	1	3	13855.984(2)	0.008
2	0	2	3	0	3	14492.409(2)	−0.004
2	1	1	3	1	2	15235.540(2)	0.004
$\text{H}_3^{15}\text{N}-\text{H}^{14}\text{NO}_3$							
0	0	0	1	0	1	4705.563(3)	0.008
1	1	1	2	1	2	8978.102(3)	−0.010
1	0	1	2	0	2	9397.104(3)	0.012
1	1	0	2	1	1	9843.937(2)	−0.004
2	1	2	3	1	3	13458.466(2)	0.001
2	0	2	3	0	3	14060.699(3)	−0.003
$\text{H}_3^{14}\text{N}-\text{H}^{15}\text{NO}_3$							
0	0	0	1	0	1	4838.030(3)	0.021
1	1	1	2	1	2	9218.549(2)	−0.008
1	0	1	2	0	2	9660.305(2)	0.023
1	1	0	2	1	1	10133.351(2)	−0.012
2	1	2	3	1	3	13818.080(3)	−0.003
2	0	2	3	0	3	14451.203(2)	−0.006
2	1	1	3	1	2	15189.898(3)	0.002
$\text{H}_3^{14}\text{N}-\text{D}^{14}\text{NO}_3$							
1	1	1	2	1	2	9160.586(1)	0.003
1	0	1	2	0	2	9601.307(2)	−0.016
1	1	0	2	1	1	10073.581(1)	0.001
2	1	2	3	1	3	13731.082(2)	−0.001
2	0	2	3	0	3	14362.532(2)	0.005

^a All frequencies in MHz. ^b Uncertainties are one standard error in the fits to quadrupole coupling constants and line centers. ^c Residuals from fits to eq 2.

in the immediate vicinity of any of the transitions observed in this work. It is worth noting that in $\text{Ar}-\text{CH}_3\text{Cl}$, for example, in which the methyl group undergoes nearly free internal rotation, transitions in the excited internal rotor state are displaced as much as several gigahertz from the corresponding transitions in the ground state.²⁶ In all of the spectral searching associated with this study,²⁷ only a single unidentified transition that appeared to require both NH_3 and HNO_3 was found. This line was not readily assigned either using ground-state constants or on the basis of hyperfine structure and may indeed belong to the excited internal rotor state. Further searches for the excited state, however, were not pursued.

Structure Analysis

The rotational constants for the four isotopic derivatives studied contain structural information about the dimer, though, clearly, the system is complex enough that a complete determination of all atomic coordinates is not possible. To simplify the problem, we make several reasonable assumptions. First, we take the heavy atom frame to be planar. This is realistic on the basis of (a) the small inertial defect of $-0.8 \text{ amu } \text{\AA}^2$ obtained from the observed rotational constants, (b) the results of ab initio theory,¹⁵ and (c) simple chemical intuition. Second, we assume (at least at the outset) that the structures of the NH_3 and HNO_3 subunits are unchanged upon complexation. It should be noted that in this case, the approximation is not rigorously supported by theory,¹⁵ which instead predicts small but significant changes in monomer geometries upon complexation. Nevertheless, it provides a useful starting point for the analysis, and the resulting preliminary structure can be appropriately modified once the method of analysis has been established.

TABLE 4: Spectroscopic Constants for H₃N–HNO₃^{a,b}

constant	H ₃ ¹⁴ N–H ¹⁴ NO ₃	H ₃ ¹⁵ N–H ¹⁴ NO ₃	H ₃ ¹⁴ N–H ¹⁵ NO ₃	H ₃ ¹⁴ N–D ¹⁴ NO ₃
<i>A</i>	12438.2(4)	12437.2(5)	12423.9(5)	12318.8(8)
<i>B</i>	2656.0627(4)	2569.2614(9)	2647.7191(6)	2632.5700(8)
<i>C</i>	2195.9697(4)	2136.3070(9)	2190.3002(6)	2176.0235(8)
Δ _J	0.003999(8)	0.00344(3)	0.00245(1)	0.00330(4)
δ _J	0.00175 ^c	0.00125 ^c	0.00050 ^c	0.00150 ^c
eQq _{aa} (NH ₃)	−1.9872(34)		−1.9817(42)	−1.9966(46)
[eQq _{bb} − eQq _{cc}](NH ₃)	−1.3334(78)		−1.336(11)	−1.3487(90)
eQq _{aa} (HNO ₃)	−0.3725(34)	−0.3724(42)		−0.3570(42)
[eQq _{bb} − eQq _{cc}](HNO ₃)	0.025 ^c	0.025(11)		0.025 ^c

^a All values in MHz. ^b Values in parentheses are one standard error in the least squares fits. ^c Constrained in fit. See text for discussion.

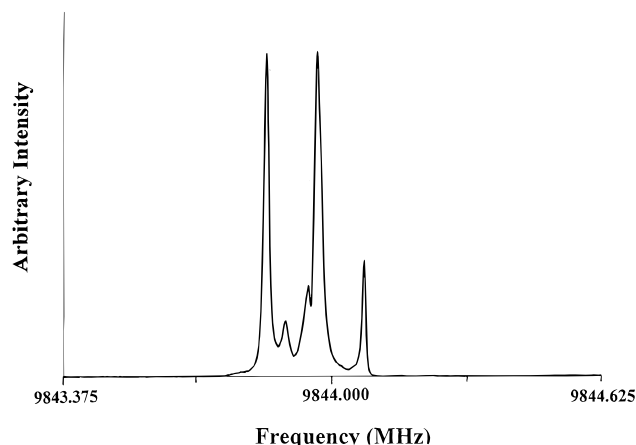


Figure 1. Power spectrum of the 1₀–2₁₁ transition of H₃¹⁵N–H¹⁴NO₃. Hyperfine components shown are (from left to right): (*F'*, *F*) = (1, 2), (2, 2), (1, 1), (2, 3), and (0, 1). This figure represents a total signal collection time of 53 s.

Assuming that the heavy atom frame is planar, the coordinates that define the structure of the complex are shown in Figure 2. *R*_{cm} is the distance between the centers of mass of the ammonia and nitric acid subunits and *γ* is the angle that the *C*₃ axis of the ammonia makes with *R*_{cm}. *θ* is the angle formed between *R*_{cm} and the *a*-inertial axis of the nitric acid. In terms of these coordinates, the moments and products of inertia in the (*X*, *Y*, *Z*) axis system shown are given by

$$I_{XX} = I_{bb}(\text{NH}_3) \sin^2 \gamma + I_{cc}(\text{NH}_3) \cos^2 \gamma + I_{bb}(\text{HNO}_3) \sin^2 \theta + I_{aa}(\text{HNO}_3) \cos^2 \theta \quad (3)$$

$$I_{YY} = M_s R_{cm}^2 + I_{bb}(\text{NH}_3) \cos^2 \gamma + I_{cc}(\text{NH}_3) \sin^2 \gamma + I_{bb}(\text{HNO}_3) \cos^2 \theta + I_{aa}(\text{HNO}_3) \sin^2 \theta \quad (4)$$

$$I_{ZZ} = M_s R_{cm}^2 + I_{bb}(\text{NH}_3) + I_{cc}(\text{HNO}_3) \quad (5)$$

$$I_{XY} = I_{YX} = [I_{cc}(\text{NH}_3) - I_{bb}(\text{NH}_3)] \sin \gamma \cos \gamma + [I_{aa}(\text{HNO}_3) - I_{bb}(\text{HNO}_3)] \sin \theta \cos \theta \quad (6)$$

$$I_{XZ} = I_{ZX} = I_{YZ} = I_{ZY} = 0 \quad (7)$$

These equations are readily derived from the transformation properties of the inertial tensor, though the angle-independent eq 5 follows directly from the parallel axis theorem.²⁸ The *I*_{gg}'s are the moments of inertia of the indicated monomers about their g-inertial axes and *M*_s is the pseudodiatom reduced mass, given by *m*(NH₃)/[*m*(NH₃) + *m*(HNO₃)].

It is important to note that with a freely or near-freely rotating NH₃ unit within the complex, the *A* and *B* rotational constants determined from eq 2 are effective constants. The *C* rotational constant, however, is independent of the internal rotation and

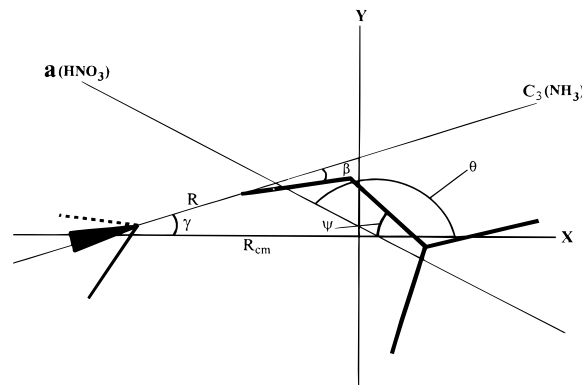


Figure 2. Definition of coordinates used to describe the structure of H₃N–HNO₃.

is simply related to the moment of inertia.^{26,29} If the heavy atom frame of the complex is planar, the inertial axis system is obtained from the (*X*, *Y*, *Z*) system of Figure 2 by rotation about *Z* and hence *C* = *h*²/8π²*I*_{ZZ} = *h*²/8π²*I*_{cc}. Moreover, since *I*_{ZZ} is independent of angles, the observed value of *C* gives *R*_{cm} directly. Values of *R*_{cm} obtained from eq 5 using the moments of inertia of free NH₃³⁰ and HNO₃³¹ are given in Table 5. Throughout the table, the upper member of each pair of numbers corresponds to that deduced using the moments of inertia of uncomplexed monomers, as discussed in more detail later on.

Although *R*_{cm} is the simplest quantity to determine, it is not the most chemically useful. Indeed, what we would like to know is the length and degree of linearity of the hydrogen bond. These parameters are specified by *R* and *β*, which are also shown in Figure 2. Clearly, with the center of mass separation determined, angular information is needed to obtain these quantities but, for reasons discussed below, hyperfine structure turns out not to provide an unambiguous approach. Thus, the rotational constants provide the only recourse.

The *A* and *B* rotational constants are indeed angle-dependent, but as noted above, their fitted values depend on the internal rotation. For free internal rotation, the effective constants determined from eq 2 are given by^{26,29}

$$A = (1 + \lambda_a^2 I_{\alpha} / r I_{aa}) (h^2 / 8\pi^2 I_{aa}) \quad (8)$$

and

$$B = (1 + \lambda_b^2 I_{\alpha} / r I_{bb}) (h^2 / 8\pi^2 I_{bb}) \quad (9)$$

where

$$r = 1 - \lambda_a^2 I_{\alpha} / I_{aa} - \lambda_b^2 I_{\alpha} / I_{bb} \quad (10)$$

*I*_α is the moment of inertia of the top about its symmetry axis, *I*_{aa} and *I*_{bb} are the rigid-molecule moments of inertia of the complex about its *a*- and *b*-inertial axes, respectively, and the

TABLE 5: Derived Parameters for H₃N–HNO₃^a

	H ₃ ¹⁴ N–H ¹⁴ NO ₃	H ₃ ¹⁵ N–H ¹⁴ NO ₃	H ₃ ¹⁴ N–H ¹⁵ NO ₃	H ₃ ¹⁴ N–D ¹⁴ NO ₃	ab initio ^b
<i>R</i> _{cm} (Å)	3.319761 3.326026	3.316506 3.322502	3.320857 3.327157	3.303981 3.308159	3.303979 ^c
<i>θ</i> (deg)	145.60 140.10	145.65 140.16	145.67 140.16	152.29 149.69	145.3 ^c
<i>R</i> (Å)	1.6736 1.7991	1.6731 1.7983	1.6714 1.7974	1.7162 1.7637	1.684
<i>β</i> (deg)	−9.8 7.3	−9.8 7.2	−10.0 7.1	−6.7 4.2	1.5
<i>ψ</i> (deg)	50.0 57.6	50.0 57.5	49.9 57.5	52.0 55.9	53.4
<i>γ</i> _e (deg)	18.1 24.6	18.1 24.6	18.0 24.5	19.2 23.1	23.4
<i>R</i> _{N–N} (Å)	3.3487 3.3319	3.3490 3.3319	3.3485 3.3321	3.3567 3.3417	3.3221 ^{c,d}

Preferred Values
 $R = 1.736 \pm 0.063$ Å
 $\beta = -1 \pm 9^\circ$
 $\psi = 54 \pm 4^\circ$
 $\gamma_e = 21 \pm 3^\circ$
 $R_{N-N} = 3.344 \pm 0.012$ Å

^a The upper member of each pair of numbers is that derived using the experimental moments of inertia of the free monomers. Lower numbers are obtained using corrected moments of inertia derived from the ab initio monomer distortions of ref 15. See text for discussion. ^b Reference 15. ^c Calculated for H₃¹⁴N–H¹⁴NO₃. ^d See footnote 34.

λ 's are the direction cosines of the top axis with respect to the indicated inertial axes.^{26,29} Using any reasonable structure for the dimer, the correction to *A* implied by eq 8 is expected to be large (>700 MHz) while that for *B* (eq 9) is small (a few megahertz). Thus, the *B* rotational constants were used to determine *R* and *β*, as described below.

The *a*-inertial axis of the complex lies within 1° of the line joining the centers of mass. Moreover, the angle-dependent terms arising from the NH₃ in eqs 3–6 are much smaller than those arising from the HNO₃. Thus, for the purpose of determining *θ*, the values of $\langle \cos^2 \gamma \rangle$ and $\langle \sin^2 \gamma \rangle$ were fixed to those determined from the ¹⁴N hyperfine structure of the ammonia subunit, viz.

$$eQq(^{14}\text{NH}_3)^{\text{complex}} = eQq(^{14}\text{NH}_3)^{\text{free}}(3\langle \cos^2 \gamma \rangle - 1)/2 \quad (11)$$

Although the quadrupole coupling constant of the ammonia may arguably differ from the free-molecule value due to electronic rearrangement, the ammonia-dependent terms enter into the equations as small corrections and the use of eq 11 should be adequate. Using the value of $eQq(^{14}\text{N})^{\text{free}} = -4.08983(2)$ MHz,³² the value of $\langle \cos^2 \gamma \rangle$ obtained is 0.657, corresponding to an effective value of $\gamma_{\text{eff}} \equiv \cos^{-1}(\langle \cos^2 \gamma \rangle^{1/2}) = 35.8^\circ$.

To obtain a first approximation to the structure of the complex, *I*_{XX}, *I*_{YY}, and *I*_{XY} were calculated for each isotopomer according to eqs 3, 4, and 6 using the values of *R*_{cm} and $\langle \cos^2 \gamma \rangle$ determined above (together with the moments of inertia of free NH₃³⁰ and HNO₃³¹). *I*_{aa} and *I*_{bb} were then obtained by rotation about *Z*, and the value of *θ* was iteratively adjusted until the calculated value of $B = h^2/8\pi^2 I_{bb}$ matched the effective value determined from experiment. Assuming that the *C*₃ axis of the ammonia is directed along the hydrogen bond, *R* and *β* were then readily obtained using the known structural parameters of the monomers. Values of *γ*_e and *ψ* were also calculated, where *γ*_e is the angle that the *C*₃ axis of the NH₃ makes with *R*_{cm} when directed toward the HNO₃ hydrogen, and *ψ* is the acute angle formed between the NO single bond and *R*_{cm}.

Next, with a preliminary structure in hand, the direction cosines appearing in eqs 8–10 were calculated and used to correct the *B* rotational constants for internal rotation. The corrections varied slightly between isotopomers, but in all cases

were less than 7.6 MHz. The calculation of the structure was then repeated to give refined parameters and the process iterated until the calculated structure was well converged to within the estimated uncertainties (about four times). The results are reported in Table 5. Also included in the table are the corresponding values derived from the theoretical work of Nguyen et al.¹⁵ Again, the upper values correspond to those obtained using the free-monomer moments of inertia.

An interesting feature of the theoretical work on this complex is that the hydrogen bond is strong enough to induce significant changes in the monomer geometries upon complexation. The calculations above, however, employ the experimental moments of inertia of the *free* monomers and hence are potentially subject to systematic errors. Thus, to estimate the magnitude of errors incurred, we calculated the fractional changes in the rotational constants of the HNO₃ and NH₃ subunits, which arise due to the theoretically determined distortions. These fractional changes were then imposed on the experimental rotational constants³³ of the uncomplexed monomers and the structure of the complex was redetermined using the revised values. The results are given as the lower member of each pair of numbers in Table 5.

It is apparent that sizable changes in the structural parameters of the complex are obtained when the rotational constants of the distorted monomers are used in place of the experimental ones. While the magnitudes of these changes surprised us at first, they can be understood as arising from a combination of several factors. First, due to the unusual strength of the NH₃–HNO₃ interaction, the distortion of the nitric acid is unusually large¹⁵ and correspondingly produces significant changes in its moments of inertia (on the order of 0.3%–0.9%). Second, the nitric acid is large enough that the *θ*-dependent terms in eqs 4 and 5 are not negligible compared with *M_eR*_{cm}². Thus, significant changes in the calculated values of *R*_{cm} and *θ* accompany the use of distorted HNO₃ constants, and these, in turn, propagate in the computation of the other structural parameters.

It is unlikely that any number of isotopic substitutions would provide accurate enough atomic coordinates for the HNO₃ to allow a redetermination of its structure within the complex. Thus, to partially circumvent the effects of distortion of the HNO₃ unit, values of the nitrogen–nitrogen distance (*R*_{N–N})

are also listed in Table 5. Since both nitrogens lie near the centers of mass of their respective monomer units, this quantity is relatively insensitive to the angular orientation of the moieties and correspondingly is much less sensitive to changes in the HNO₃ internal structure. Indeed the consistency among the various determinations is seen to be significantly better than that among determinations of R.

In the case of H₂O–HNO₃,³⁵ we argued that the calculated changes in the monomer geometries upon complexation³⁶ represented an upper limit to the true changes because only the energies (not the structures) had been corrected for basis set superposition error (BSSE). Although the calculations on H₃N–HNO₃ used a bigger basis set, and BSSE corrections were therefore not applied, there is an additional reason to suppose that the calculated changes may be taken as upper limits here as well. In particular, the calculated monomer distortions refer to those in the complex at its *equilibrium configuration*, i.e., the structure corresponding to the strongest interaction. Zero point motion along the van der Waals coordinates, however, would presumably act to reduce the effective degree of distortion as the moieties' orientations are averaged over configurations of weaker interaction. Thus, even apart from BSSE, the structural results obtained using the “fully distorted” HNO₃ geometry probably represent a worst-case scenario in terms of the effect of these distortions on the computed structure of the complex.

In light of these arguments, we expect that the true structural parameters of H₃N–HNO₃ lie between those computed without regard to distortion of the monomers and those obtained using the fully distorted geometries. Thus, the “preferred values” are taken as the median of the set of determinations represented in Table 5, with uncertainties chosen to encompass the results of all determinations. These results are also presented in Table 5.

Discussion

It is apparent that the observed structure of the complex is in extraordinary agreement with that calculated by Nguyen et al.¹⁵ The experimental value of the hydrogen bond length, for example, differs from the theoretical result by only 0.052 ± 0.060 Å, and the remaining structural parameters also show impressive agreement. The hydrogen bond angle, β , is not determined with great accuracy but is clearly consistent with a linear or near-linear hydrogen bond. The general consistency between the observed and calculated values for these parameters supports the theoretical structure and hence the large reported binding energy of 14.3 kcal/mol. A strong hydrogen bonding interaction between nitric acid and ammonia is certainly to be expected chemically.

As noted in the previous theoretical work,¹⁵ the hydrogen bond length is unusually short. For example, the 1.736 Å bond length reported in Table 5 is significantly shorter than the 1.853 and 1.831 Å values observed in ClH–NH₃³⁷ and BrH–NH₃,³⁸ respectively, and even slightly shorter than the 1.78 Å distance reported for FH–NH₃.³⁹ Interestingly, it is also even slightly shorter than the 1.78 Å distance observed in H₂O–HNO₃,³⁵ despite the 0.1 Å increase in the van der Waals radius of nitrogen relative to oxygen.⁴⁰ This no doubt derives from the increased basicity of ammonia relative to that of water.

It is also of interest to examine the consistency of the observed ¹⁴N hyperfine structure with the geometry of the dimer determined above. Albinus et al.⁴¹ have given the orientation of the principal axis system (*x*, *y*, *z*) for the quadrupole coupling tensor in free nitric acid. With their choice of axis labeling, the *x*-axis forms an angle of 16.6° with the *a*-axis of H¹⁴NO₃,

placing it at 1.1° with respect to the N–O single bond, rotated away from the hydrogen. From the structure of the complex determined above, therefore, we calculate that the *x*-axis of the quadrupole coupling tensor forms an angle of $\phi = 54^\circ$ with the *a*-inertial axis of the complex.

Assuming that the complex is planar and that the quadrupole coupling tensor of HNO₃ is unperturbed by the interaction with NH₃, the values of (*eQq_{aa}*) and (*eQq_{bb}* – *eQq_{cc}*) for the HNO₃ subunit are given by

$$eQq_{aa} = eQq_{xx} \cos^2 \phi + eQq_{yy} \sin^2 \phi \quad (12)$$

and

$$[eQq_{bb} - eQq_{cc}] = (eQq_{xx})(1 + \sin^2 \phi) + (eQq_{yy})(1 + \cos^2 \phi) \quad (13)$$

where *eQq_{xx}* and *eQq_{yy}* are in the in-plane eigenvalues of the quadrupole coupling tensor of free nitric acid.⁴¹ Using the literature values *eQq_{xx}* = 1.103(19) MHz and *eQq_{yy}* = –1.033(21) MHz,⁴¹ we thus determine that the observed value of *eQq_{aa}* for the complex implies a value of $\phi = 56^\circ$. The agreement with the 54° value quoted above is excellent. The value of [*eQq_{bb}* – (*eQq_{cc}*)] , however, implies a value of $\phi = 43^\circ$, which is in somewhat poorer agreement with that determined from the structure. Moreover, we find that there is no value of ϕ that can simultaneously reproduce both *eQq_{aa}* and [*eQq_{bb}* – *eQq_{cc}*]. Thus, while *eQq_{aa}* supports the structure determined from rotational constants, we could find no independently justifiable means of choosing it over [*eQq_{bb}* – *eQq_{cc}*] for use in the structural analysis and it is for this reason that the structure was determined using only the rotational constants.

Some further insight into the possible implications of the observed hyperfine parameters can be obtained. To the extent the complex is planar and the monomers unperturbed, *eQq_{cc}* for the HNO₃ nitrogen should equal that of free nitric acid (–0.070 ± 0.008 MHz⁴¹). From the coupling constants given in Table 4, however, (and the supplementary condition that *eQq_{aa}* + *eQq_{bb}* + *eQq_{cc}* = 0), we determine that the experimental value of *eQq_{cc}*(HNO₃) for the complex is equal to +0.174(7) MHz. This implies either a significant change in the quadrupole coupling tensor of HNO₃ upon complexation or some degree of zero point oscillation of the HNO₃ unit out of the molecular plane (or both). If electronic effects within a planar complex were the sole cause, we would conclude that $\Delta(eQq_{xx}) + \Delta(eQq_{yy}) = -0.244(15)$ MHz, where the Δ 's refer to change upon complexation. This follows since $\Delta(eQq_{cc}) \equiv eQq_{cc}(\text{complex}) - eQq_{cc}(\text{HNO}_3) = \Delta(eQq_{zz}) = -[\Delta(eQq_{xx}) + \Delta(eQq_{yy})]$.

Distinguishing electronic rearrangement from zero point oscillation effects, however, is not easily done in this system. Nevertheless, it is interesting to compare *eQq_{cc}* for H₃N–HNO₃ with that derived from the previously published quadrupole coupling constants of H₂O–HNO₃.³⁵ For that complex, we calculate a value of *eQq_{cc}* of 0.075 MHz, which is not equal to but is certainly closer to that of free nitric acid than is *eQq_{cc}* of H₃N–HNO₃. Interestingly, in HCl–HNO₃ (where the hydrogen bonding should be even weaker), preliminary analysis⁴² gives a value of *eQq_{cc}* equal to 0.047 MHz. Since the vibrational amplitudes of the nitric acid should not be too different in these three systems, the correlation between *eQq_{cc}* and base strength would appear to indicate that electronic distortion is significant, at least in the NH₃ complex. Such a conclusion is reasonable

in light of similar observations for the R_3N-HX complexes¹⁴ and, more recently, even weakly bound complexes of N_2O .⁴³

Conclusions

Microwave spectra of four isotopomers of H_3N-HNO_3 have been obtained by Fourier transform spectroscopy. The spectra are consistent with a planar heavy-atom frame and the formation of a linear or near-linear hydrogen bond involving the lone pair on the ammonia and the acidic proton of the nitric acid. The hydrogen bond length is 1.736(63) Å. The NO single bond of the nitric acid forms an angle of 54(4)° with the line joining the centers of mass of the monomer units, and the C_3 axis of the ammonia is oriented at 21(3)° with respect to the same line. The nitrogen–nitrogen distance, which is the most accurately determined structural parameter in this study, is 3.344(12) Å.

The experimental structure is in excellent agreement with recent ab initio studies¹⁵ that give a binding energy of 14.3 kcal/mol. The hydrogen bond distance is exceptionally short and is consistent with the large calculated binding energy. The ^{14}N nuclear hyperfine structure suggests significant electronic distortion of the nitric acid upon complexation, but the degree of distortion is difficult to separate quantitatively from zero point averaging effects.

Acknowledgment. This work was supported by the National Science Foundation and the donors of the Petroleum Research Fund, administered by the American Chemical Society. We are also grateful to Professor Fu-Ming Tao for a preprint of ref 15 and for his patience and insights during several valuable discussions.

References and Notes

- (1) Kramm, G.; Dlugi, R. *J. Atmos. Chem.* **1994**, *18*, 319.
- (2) Dentener, F. J.; Crutzen, P. J. *J. Atmos. Chem.* **1994**, *19*, 331.
- (3) Brost, R. A.; Delany, A. C.; Huebert, B. J. *J. Geophys. Res.* **1988**, *93* (D6), 7137.
- (4) Harrison, R. M.; Rapsomanikis, S.; Turnbull, A. *Atmos. Environ.* **1989**, *23*, 1795.
- (5) Langford, A. O.; Fehsenfeld, F. C.; Zachariassen, J.; Schimel, D. S. *Global Biogeochem. Cycles* **1992**, *6*, 459.
- (6) Stelson, A. W.; Friedlander, S. K.; Seinfeld, J. H. *Atmos. Environ.* **1979**, *13*, 369.
- (7) Tang, I. N. *Atmos. Environ.* **1980**, *14*, 819.
- (8) Stelson, A. W.; Seinfeld, J. H. *Atmos. Environ.* **1982**, *16*, 993.
- (9) Raes, F.; Kudas, T. T.; Friedlander, S. K. *Aerosol Sci. Technol.* **1990**, *12*, 856.
- (10) Lammel, G.; Pohlmann, G. *J. Aerosol Sci.* **1992**, *23*, Suppl 1, S941.
- (11) Ritzhaupt, G.; Devlin, J. P. *J. Phys. Chem.* **1977**, *81*, 521.
- (12) (a) Ritzhaupt, F.; Devlin, J. P. *J. Chem. Phys.* **1991**, *95*, 90. (b) Barnes, A. J.; Lasson, E.; Nielsen, C. J. *J. Mol. Struct.* **1994**, *322*, 165.
- (13) See, for example: (a) Pimentel, G. C.; McClellan, A. L. *The Hydrogen Bond*; W. H. Freeman: San Francisco, 1960 (see also references therein). (b) Clementi, E. *J. Chem. Phys.* **1967**, *46*, 3851. (c) Goldfinger, P.; Verhaegen, G. *J. Chem. Phys.* **1969**, *50*, 1467. (d) Ault, B. S.; Pimentel, G. C. *J. Phys. Chem.* **1973**, *77*, 57. (e) Ault, B. S.; Pimentel, G. C. *J. Phys. Chem.* **1973**, *77*, 1649.
- (14) Legon, A. C. *Chem. Soc. Rev.* **1993**, 153 and references therein.
- (15) Nguyen, M.-T.; Jamka, A. J.; Cazar, R. A.; Tao, F.-M. *J. Chem. Phys.* **1997**, *106*, 8710.
- (16) Tao, F.-M. *J. Chem. Phys.* **1998**, *108*, 193.
- (17) Cazar, R. A.; Jamka, A. J.; Tao, F.-M. *J. Phys. Chem.* **1998**, *102*, 5117.
- (18) Latajka, Z.; Szczesniak, M. M.; Ratajczak, H.; Orville-Thomas, W. *J. J. Comput. Chem.* **1980**, *1*, 417.
- (19) Balle, T. J.; Flygare, W. H. *Rev. Sci. Instrum.* **1981**, *52*, 33.
- (20) (a) Phillips, J. A.; Canagaratna, M. Goodfriend, H.; Grushow, A.; Almlöf, J.; Leopold, K. R. *J. Am. Chem. Soc.* **1995**, *117*, 12549. (b) Phillips, J. A. Ph.D. Thesis, University of Minnesota, 1996.
- (21) (a) Legon, A. C.; Wallwork, A. L.; Rego, C. A. *J. Chem. Phys.* **1990**, *92*, 6397. (b) Lovas, F. J.; Suenram, R. D.; Fraser, G. T.; Gillies, C. W.; Zozom, J. J. *J. Chem. Phys.* **1988**, *88*, 722. (c) Gutowsky, H. S.; Chen, J.; Hajduk, P. J.; Keen, J. D.; Emilsson, T. *J. Am. Chem. Soc.* **1989**, *111*, 1901. (d) Emilsson, T.; Klotz, T. D.; Ruoff, R. S.; Gutowsky, H. S. *J. Chem. Phys.* **1990**, *93*, 6971.
- (22) Chilton, T. H. *Strong Water Nitric Acid: Sources, Methods of Manufacture, and Uses*; MIT Press: Cambridge, 1968; p 166.
- (23) (a) Townes, C. H.; Schawlow, A. L. *Microwave Spectroscopy*; Dover: New York, 1975. (b) Gordy, W.; Cook, R. L. *Microwave Molecular Spectra*; John Wiley and Sons: New York, 1984. (c) Robinson, G. W.; Cornwell, C. D. *J. Chem. Phys.* **1953**, *21*, 1436.
- (24) This procedure was necessary because the small value of δJ produced singular matrices in our Gauss–Jordan matrix inversion subroutine, causing the least squares fit to terminate.
- (25) During the preparation of this manuscript, Prof. F.-M. Tao kindly calculated the internal rotation barrier for us. The value obtained, 31.3 cm^{-1} , is indeed low.
- (26) Fraser, G. T.; Suenram, R. D.; Lovas, F. J. *J. Chem. Phys.* **1987**, *86*, 3107.
- (27) This searching includes the 4300–6100 and 9500–10 600 MHz ranges noted above as well as approximately 500 MHz on either side of the $0_{00}-1_{01}$ transition of the parent isotopomer.
- (28) Symon, K. R. *Mechanics*, 3rd ed.; Addison-Wesley: Reading, MA, 1971.
- (29) Kilb, R. W.; Lin, C. C.; Wilson, E. B., Jr. *J. Chem. Phys.* **1957**, *26*, 1695.
- (30) Helminger, P.; De Lucia, F. C.; Gordy, W. *J. Mol. Spectrosc.* **1971**, *39*, 94.
- (31) (a) Cox, A. P.; Riveros, J. M. *J. Chem. Phys.* **1965**, *42*, 3106. (b) Millen, D. J.; Morton, J. R. *J. Chem. Soc.* **1960**, 1523.
- (32) Marshall, M. D.; Muenter, J. S. *J. Mol. Spectrosc.* **1981**, *85*, 322.
- (33) This procedure has the advantage that it avoids errors associated with the failure of the published structure of HNO_3 to accurately reproduce its observed moments of inertia.
- (34) There appears to be an error in the N–N distance reported in ref 15. We use here the corrected value for the published theoretical structure.
- (35) Canagaratna, M.; Phillips, J. A.; Ott, M. E.; Leopold, K. R. *J. Phys. Chem.* **1998**, *102*, 1489.
- (36) Tao, F.-M.; Higgins, K.; Klemperer, W.; Nelson, D. D. *Geophys. Res. Lett.* **1996**, *23*, 1797.
- (37) Howard, N. W.; Legon, A. C. *J. Chem. Phys.* **1988**, *88*, 4694.
- (38) Howard, N. W.; Legon, A. C. *J. Chem. Phys.* **1987**, *86*, 6722.
- (39) Calculated from the N–F distance of B. J. Howard and P. R. R. Langridge-Smith, quoted in ref 14.
- (40) Cotton, F. A.; Wilkinson, G. *Advanced Inorganic Chemistry*, 3rd ed.; Interscience: New York, 1972.
- (41) Albinus, L.; Spieckermann, J.; Sutter, D. H. *J. Mol. Spectrosc.* **1989**, *133*, 128.
- (42) Ott, M. E.; Leopold, K. R. Manuscript in preparation.
- (43) (a) Leung, H. O. *J. Chem. Phys.* **1998**, *108*, 3955. (b) Leung, H. O.; Gangwani, D.; Grabow, J.-U. *J. Mol. Spectrosc.* **1997**, *184*, 106.